Hierarchical Assembly of CuO Nano-Dandelions on 3-D Printed Template

Md Didarul Islam,[1] Hamad Al Yassi,[2] Mengyao Dong,[3] Daniel S. Choi,[2] Ilwoo Seok,[4] Chuntai Liu,[5] Zhanhu Guo[3] and Jong Eun Ryu[1*]

We report a two-phase chemical synthesis of various copper (Cu) nanostructures throughout complex 3-dimensional (3-D) printed substrates. We present dandelion-like CuO nano-rods grown on a 3-D model. 1 mm x 1 mm x 10 mm bars are cross-stacked to form a cubic log-pile structure. Ni thin-film was electrolessly deposited, and subsequently Cu layer was electroplated on the 3-D log-pile structure. In order to grow nanostructures, the Cu layer was reacted with an alkali solution (NH_4OH). The surface morphology and chemistry were characterized by field emission scanning electron microscopy (SEM) and energy-dispersive X-ray spectroscopy (EDX).

1. Introduction

Additive manufacturing, popularly known as 3-dimensional (3-D) printing, is a process that creates parts by continuously adding material layer by layer. This technique has been utilized to create complex structures, such as internal hierarchal patterns, which are impossible to create with other conventional manufacturing methods.[1] Since inception, 3-D printing technology has found wide application areas, including rapid prototyping in manufacturing,[2] tissue engineering,[3-5] and prosthetics.[6] The 3-D models are fabricated by various methods, for example, fused deposition,[7] binder jet,[8,9] laser sintering,[10] and stereolithography.[11] However, fundamental roles of those 3-D printed models are commonly limited to mechanical load bearing structures or supporting matrices. As the technology has matured in terms of printing quality and printable materials, the 3-D printing technology has led a shift in future manufacturing paradigm from centralized mass-production to customized local low-volume manufacturing, which is suitable for the customized end-use products.[12-13] The next evolution of 3-D printing will be to integrate complex electronics functionality into the 3-D manufacturing process, which can create novel end-use products in various areas, such as the wearable electronics (e.g.

computers and cell-phones) and the augmented prosthesis shaped to fit a specific users' anatomy. Therefore, there is an urgent need to develop printable functional materials and functionalized printed materials.

Nanomaterials, such as nanoparticles and nanowires, have been utilized for functionalization of substrates through various methods including chemical growth,[14,15] physical deposition,[16,17] and adsorption.[18] For example, noble metal nanoparticles (e.g. Au, Pt, Pd, Ru) immobilized on conductive substrates were used as electrochemical glucose monitors[14,15,19] and gas sensors.[20] Furthermore, energy storage devices, such as Li-ion batteries[21-28] and capacitors,[29-35] showed high energy and power density due to the large specific area of nanomaterials. Recently, nanoparticles of $Li_4Ti_5O_{12}$ and $LiFePO_4$ were mixed with polymer resins, and a micro Li-ion battery was fabricated by a 3-D printer, which overlays thin layers of the resins for anode and cathode of the battery, respectively.[36] However, until today, functional materials in different material classes, such as polymers and metals, have been printed through an additional secondary printer, which is known as the multiprocess approach.[37-39] In our study, instead of challenging the disadvantages in combining multiple 3-D printers that are manufactured and operated differently, we propose an alternative method to create metallic nanostructures on 3-D printed objects.

We envisioned that the multifunctional 3-D structures functionalized by nanomaterials will further enable us to design new devices, which could not be attained through the conventional micro-fabrication processes or the multiprocess 3-D printing. Our goal of this study is to establish a fabrication method for integration of nanomaterials on 3-D printed structures through a scalable and economic self-assembly.

In this research, 3-D log-pile blocks were fabricated by a UV curable polyjet printer and copper (Cu) was electrodeposited on a thin nickel (Ni) interfacial layer, which was coated through electroless deposition for conformal metallization of the 3-D models. Subsequently, the Cu deposited 3-D log-pile blocks were immersed in alkali solutions to obtain hierarchical nanostructures of Cu oxide. Successful proof-of-concept in this paper will provide a new pathway to fabricate complex 3-D structures functionalized by nanomaterials.

[1] *Department of Mechanical and Aerospace Engineering, North Carolina State University, Raleigh, NC 27695, USA*

[2] *Department of Mechanical Engineering, Khalifa University of Science and Technology, Abu Dhabi, United Arab Emirates*

[3] *Department of Chemical and Biomolecular Engineering University of Tennessee, Knoxville, TN 37996, USA*

[4] *Department of Mechanical Engineering, Arkansas State University, Jonesboro, AR 72401, USA*

[5] *Key Laboratory of Materials Processing and Mold, Ministry of Education; National Engineering Research Center for Advanced Polymer Processing Technology, Zhengzhou University, Zhengzhou, 450002, China*

***E-mail:** jryu@ncsu.edu*

2. Experimental section

With a 3-D polyjet printer (Stratasys, Objet500Connex), we printed rigid UV curable polymer (VeroWhite®) into a 3-D log-pile structure. 1 mm x 1 mm x 10 mm bars are cross-stacked to form a 1 cm x 1 cm x 1 cm cubic structure (Fig. 1). Electroless Ni plating was performed as described in the literature[40,41] using plating solutions manufactured by MacDermid Industrial, USA. The 3-D log-pile block was immersed in an acidic etchant at 80 °C for 10 min. Pd metal salt was adsorbed by chemisorption mechanism[42] on the surface by dipping the block into a catalyst solution bath, which is composed of 0.5 g/L palladium chloride (PdCl) and 3 mL/L hydrochloric acid (HCl), for 3 min at the room temperature. Subsequently, the 3-D substrate surface was activated by Pd catalytic nuclei, which was formed in an activator solution bath at 50°C for 1 min. Finally, electroless Ni plating was performed in a plating solution containing nickel chloride (NiCl$_2$·6H$_2$O, pH=9) at 27 °C for 5 min. The 3-D printed block was rinsed with DI water after each solution treatment. Cu electroplating was performed on the Ni-plated 3-D log-pile block using a commercially available copper electroplating bath (Caswell Inc., USA). Two copper plates and 3-D printed block were connected to anode and cathode, respectively, and constant current (0.07 A) was applied for 30 min using Keithley 2400 Sourcemeter (USA). The copper plates were linearly aligned with the 3-D printed
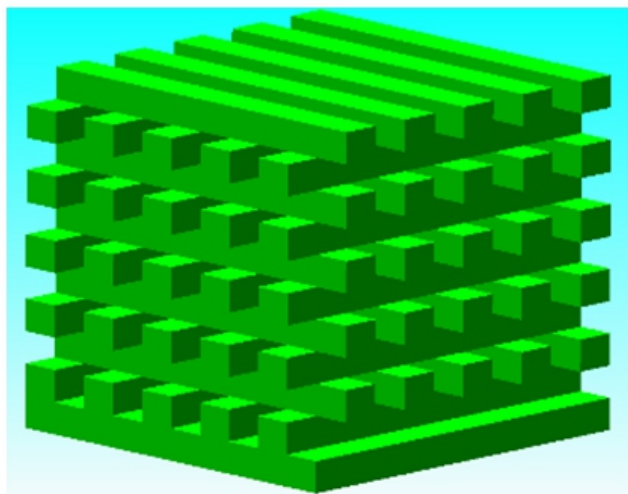
block with the same distance, and the plating solution was mildly stirred by magnetic stirrer at 30 °C. The Cu plated samples were thoroughly rinsed with DI water. Afterward, Cu plated substrates were immersed in 1M NH$_4$OH at 60 °C for nanostructure growth as described in the literatures[43-45] and allowed to react for 4 – 10 hours. Samples were then rinsed with DI water and left to air dry. Surface characterization was performed with field emission scanning electron microscopy (JEOL7800F, Japan) and energy-dispersive X-ray spectroscopy (EDAX, Japan).

3. Results and discussion

Fig. 2 shows macroscopic images of log-pile blocks after 3-D print, Ni electroless deposition, Cu electrodeposition, and surface oxidation with NH4OH for 10 hours. The samples are darkened after removal from the etchant solution and turned to complete black after Ni deposition. The samples appear orange color of pristine Cu after the electroplating. Color change due to the reaction with NH4OH occurred slowly. Noticeable change to brownish color started after 8 hours of reaction and the whole sample surface turned to brown color after 10 hours. SEM micrographs of Cu plated 3-D block after etching up to 10 hours are shown in Fig. 3.

Electroplated Cu surface shows cracks and voids as shown in Fig. 3a. The voids and cracks grow as the reaction time increased for 4 and 6 hours of etching, respectively (Figs. 3b&3c). As the reaction time increased, the mounds become easily visible and dense as shown in 10 hours etched sample in Fig. 3d. The diameters of the round mounds are distributed within 1 – 2 µm range. High magnification micrographs for the 10 hours etched sample showed sharp spikes, whose height was 50 – 100 nm, on the round mounds, and the overall shapes exhibit a dandelion-like configuration (Figs. 3e&3f). Of note, the visual appearance as well as the SEM micrographs showed the same signatures of surface morphology.

Chemical composition of each sample was confirmed by EDX (Fig. 4). Weight % of oxygen (O) increased from 8.01 % to 16.38 %, 18.30 %, and 32.98 % for as deposited Cu surface, 4 hours, 6 hours, and 10 hours etched surfaces, respectively. Nam et al. confirmed with X-ray diffraction that the surface transforms to CuO as reaction time with NH$_4$OH was increased at the same temperature (60 °C).[43] In addition, more Ni was detected than Cu in 10 hours etched sample (15.39 % of Ni and 7.22 % of Cu). This observation implies that more Ni layer was exposed as Cu etched away and formed dandelion-like structures. However, further experimental evidence will be gathered to confirm whether the nano-dandelions are copper or nickel oxide.
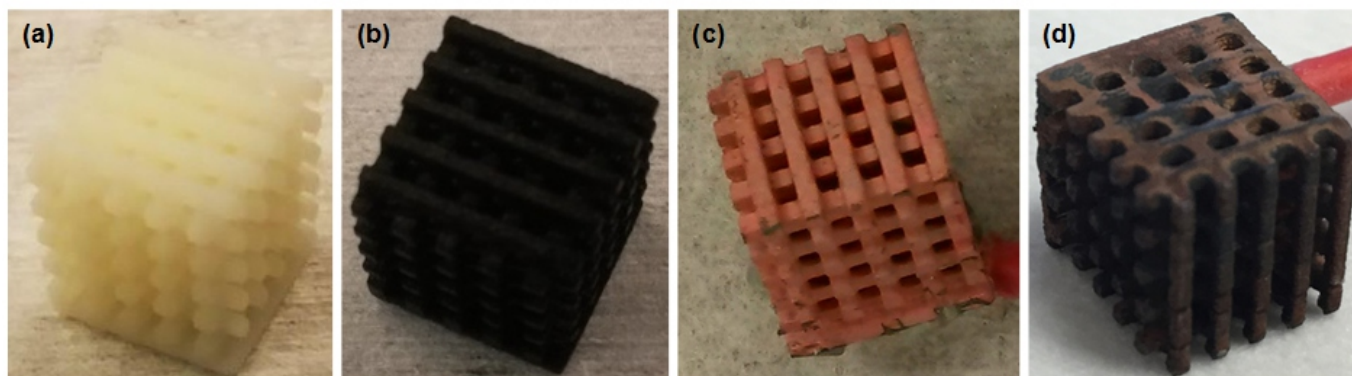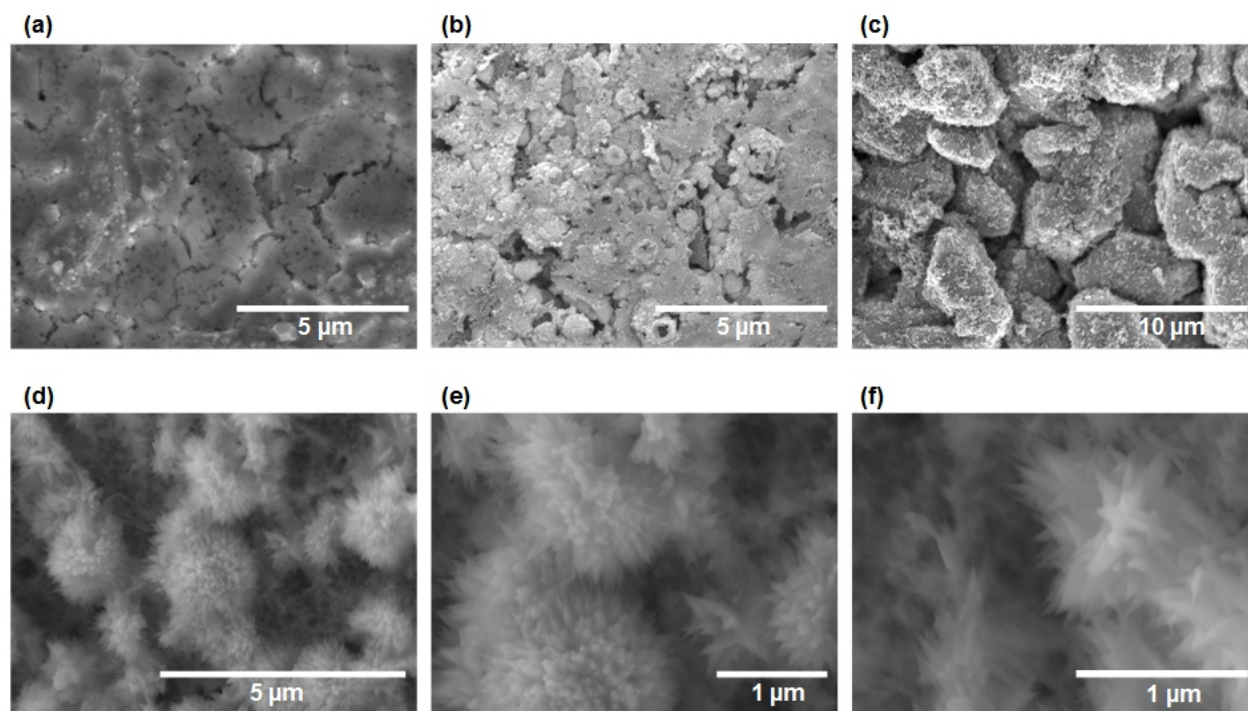

Fig. 1 3-D model of log-pile block.

Fig. 2 Macroscopic images of 3-D log-pile blocks (a) as printed (white), after (b) Ni electroless plating (black), (c) Cu electroplating (orange), and (d) 10 hours of etching in NH$_4$OH (brown).

Fig. 3 (a) As plated Cu on 3-D printed VeroWhite®; (b) – (d) After etching in 1M NH4OH at 60 °C for 4, 6 and 10 hours, respectively; (e) – (f) hierarchical nanostructure (nano dandelion) in 10 hours etched Cu.
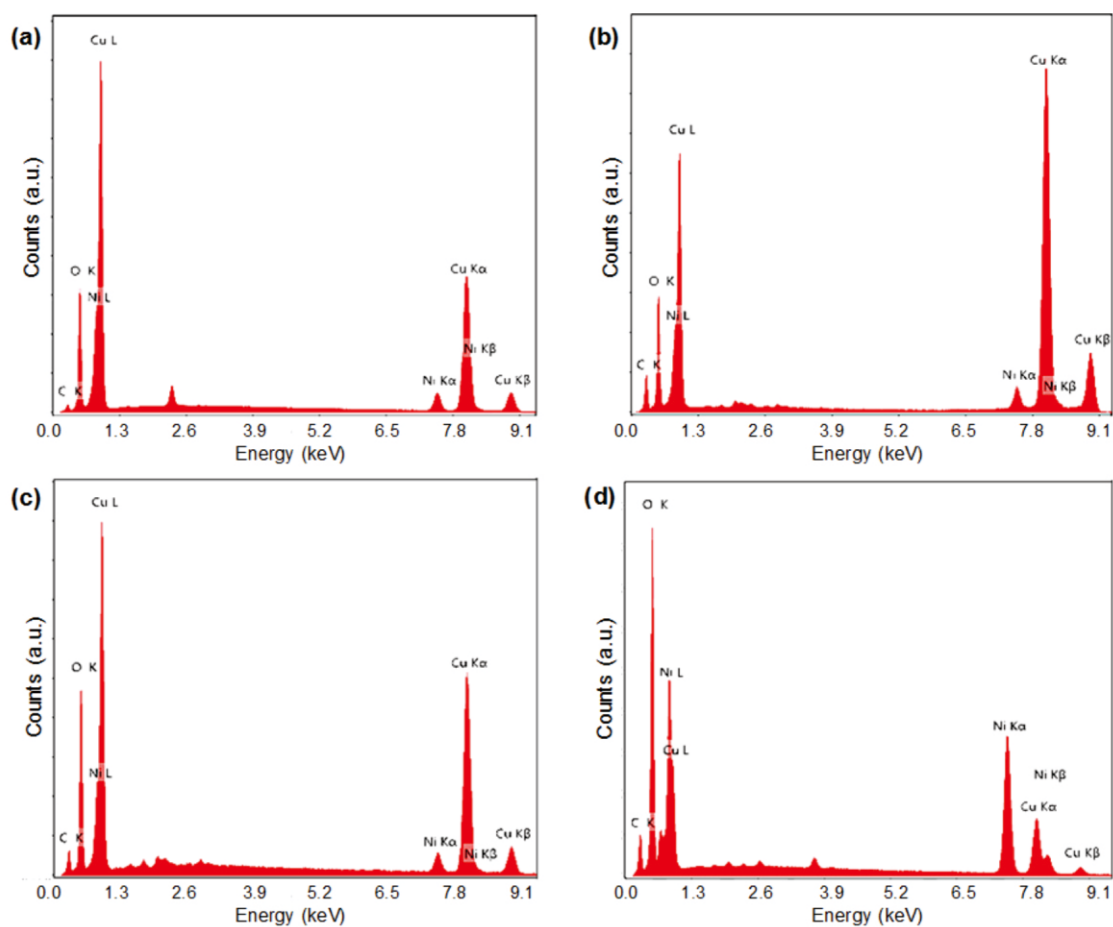
Fig. 4 EDX spectra of Cu on 3-D printed VeroWhite® after (a) 0 hour, (b) 4 hours, (c) 6 hours, and (d) 10 hours of etching with 1M NH$_4$OH at 60 °C.

4. Conclusions

This study presents a working method of forming conformal Ni and subsequent Cu metallization on 3-D printed polymer models. Further, it demonstrates hierarchical dandelion-like CuO nanostructure formation on those surfaces. It is promising that this approach allows the immense amount of research done in Cu nanostructure applications to be utilized in any printable 3-D macrostructure. Unique nano-dandelion structure is expected to increase the surface area to volume ratio, which improves the rate of reactions on surface. As one of the results, the nano-dandelion structured electrode will enhance the sensitivity and dynamic range of bio-/chemical sensors, and the power of energy conversion devices.

For our continued research, we are developing energy storage and biosensor devices based on 3-D print technology and nanostructure modification presented in this paper.

Conflict of interest

There are no conflicts to declare.

Acknowledgements

References

1. B. P. Conner, G. P. Manogharan, A. N. Martof, L. M. Rodomsky, C. M. Rodomsky, D. C. Jordan and J. W. Limperos, *Add. Manuf.*, 2014, **1-4**, 64-76.
2. E. Sachs, M. Cima, P. Williams, D. Brancazio and J. Cornie, *J. Eng. Ind.*, 1992, **114**, 481-488.
3. S. Yang, K. Leong, Z. Du and C. Chua, *Tissue Eng.*, 2002, **8**, 1-11.
4. V. Mironov, T. Boland, T. Trusk, G. Forgacs and R. R. Markwald, *Trends Biotechnol.*, 2003, **21**, 157-161.
5. M. Lee, J. C. Dunn and B. M. Wu, *Biomaterials*, 2005, **26**, 4281-4289.
6. P. Ng, P. Lee and J. Goh, *Rapid Prototyping J.*, 2002, **8**, 53-59.
7. S. J. Kalita, S. Bose, H. L. Hosick and A. Bandyopadhyay, *Mat. Sci. Eng. C*, 2003, **23**, 611-620.
8. J. E. Ryu, E. Salcedo, H. J. Lee, S. J. Jang, E. Y. Jang, H. A. Yassi, D. Baek, D. Choi and E. Lee, *J. Comp. Mat.*, 2018.
9. E. Salcedo, D. Baek, A. Berndt and J. E. Ryu, *Add. Manuf.*, 2018, **22**, 351-359.
10. J. M. Williams, A. Adewunmi, R. M. Schek, C. L. Flanagan, P. H. Krebsbach, S. E. Feinberg, S. J. Hollister and S. Das, *Biomaterials*, 2005, **26**, 4817-4827.
11. P. X. Lan, J. W. Lee, Y. Seol and D. Cho, *J. Mater. Sci. Mater. Med.*, 2009, **20**, 271-279.
12. H. Lipson and M. Kurman, John Wiley & Sons, 2013.
13. H. N. Chan, M. J. A. Tan and H. Wu, *Lab Chip*, 2017, **17**, 2713-2739.
14. H. Wu, W. Cao, Y. Li, G. Liu, Y. Wen, H. Yang and S. Yang, *Electrochim. Acta*, 2010, **55**, 3734-3740.
15. L. Lu, H. Li, F. Qu, X. Zhang, G. Shen and R. Yu, *Biosensors Bioelectron.*, 2011, **26**, 3500-3504.
16. J. Ryu, H. Kim, H. T. Hahn and D. Lashmore, *Biosensors Bioelectron.*, 2010, **25**, 1603-1608.
17. J. Ryu, K. Kim, H. Kim, H. T. Hahn and D. Lashmore, *Biosensors Bioelectron.*, 2010, **26**, 602-607.
18. X. Zhang, G. Wang, X. Liu, J. Wu, M. Li, J. Gu, H. Liu and B. Fang, *J. Phys. Chem. C*, 2008, **112**, 16845-16849.
19. F. Xiao, F. Zhao, D. Mei, Z. Mo and B. Zeng, *Biosensors Bioelectron.*, 2009, **24**, 3481-3486.
20. A. Star, V. Joshi, S. Skarupo, D. Thomas and J. P. Gabriel, *J. Phys. Chem. B*, 2006, **110**, 21014-21020.
21. K. T. Nam, D. Kim, P. J. Yoo, C. Chiang, N. Meethong, P. T. Hammond, Y. Chiang and A. M. Belcher, *Science*, 2006, **312**, 885-888.
22. Z. Wu, W. Ren, L. Wen, L. Gao, J. Zhao, Z. Chen, G. Zhou, F. Li and H. Cheng, *ACS nano*, 2010, **4**, 3187-3194.
23. M. Idrees, S. Batool, J. Kong, Q. Zhuang, H. Liu, Q. Shao, N. Lu, Y. Feng, E. K. Wujcik and Q. Gao, *Electrochim. Acta*, 2019, **296**, 925-937.
24. M. Idrees, S. Batool, Q. Zhuang, J. Kong, I. Seok, J. Zhang, H. Liu, V. Murugadoss, Q. Gao and Z. Guo, *Ceram.Int.*, 2019.
25. W. Zhao, X. Li, R. Yin, L. Qian, X. Huang, H. Liu, J. Zhang, J. Wang, T. Ding and Z. Guo, *Nanoscale*, 2019, **11**, 50-59.
26. R. Li, C. Lin, N. Wang, L. Luo, Y. Chen, J. Li and Z. Guo, *Adv. Compos. Hybrid. Mater.*, 2018,1-20.
27. H. Lyu, P. Li, J. Liu, S. Mahurin, J. Chen, D. K. Hensley, G. M. Veith, Z. Guo, S. Dai and X. Sun, *Chem. Sus. Chem.*, 2018, **11**, 763-772.
28. H. Lyu, J. Liu, S. Qiu, Y. Cao, C. Hu, S. Guo and Z. Guo, *J. Mater. Chem. A*, 2016, **4**, 9881-9889.
29. Z. Wu, W. Ren, D. Wang, F. Li, B. Liu and H. Cheng, *ACS nano*, 2010, **4**, 5835-5842.
30. W. Du, X. Wang, J. Zhan, X. Sun, L. Kang, F. Jiang, X. Zhang, Q. Shao, M. Dong and H. Liu, *Electrochim. Acta*, 2019, **296**, 907-915.
31. L. Yang, M. Shi, M. Jiang, Y. Liu, C. Yan, H. Liu and Z. Guo, *Mater. Lett.*, 2019.
32. B. Kirubasankar, V. Murugadoss, J. Lin, T. Ding, M. Dong, H. Liu, J. Zhang, T. Li, N. Wang and Z. Guo, *Nanoscale*, 2018, **10**, 20414-20425.
33. L. Liu, Q. Lu, S. Yang, J. Guo, Q. Tian, W. Yao, Z. Guo, V. A. Roy and W. Wu, *Adv. Mater. Technol.*, 2018, **3**, 1700206.
34. Y. Ma, C. Hou, H. Zhang, M. Qiao, Y. Chen, H. Zhang, Q. Zhang and Z. Guo, *J. Mater. Chem. A*, 2017, **5**, 14041-14052.
35. X. Chen, H. Wang, H. Yi, X. Wang, X. Yan and Z. Guo, *J. Phys. Chem. C*, 2014, **118**, 8262-8270.
36. K. Sun, T. Wei, B. Y. Ahn, J. Y. Seo, S. J. Dillon and J. A. Lewis, *Adv. Mater.*, 2013, **25**, 4539-4543.
37. E. MacDonald and R. Wicker, *Science*, 2016, **353**, 2093.
38. E. Aguilera, J. Ramos, D. Espalin, F. Cedillos, D. Muse, R. Wicker and E. MacDonald, 2013, 950-961.
39. D. Espalin, D. W. Muse, E. MacDonald and R. B. Wicker, *Int. J. Adv. Manuf. Technol.*, 2014, **72**, 963-978.
40. M. Schlesinger, "Electroless and electrodeposition of silver," John Wiley & Sons, Inc.: Hoboken, NJ, USA, 2010.
41. M. S. Mansouri, B. H. An, H. Al Shibli, H. Al Yassi, T. S. Alkindi, J. S. Lee, Y. K. Kim, J. E. Ryu and D. S. Choi, *Cur. Appl. Phys.*, 2018, **18**, 1235-1239.
42. J. Huang and Z. Chen, *RSC Adv.*, 2017, **7**, 25622-25626.
43. Y. Nam, S. Sharratt, C. Byon, S. J. Kim and Y. S. Ju, *J. Microelectromech. S.*, 2010, **19**, 581-588.
44. Y. Nam and Y. S. Ju, "Comparative study of copper oxidation schemes and their effects on surface wettability," 2008, 1833-1838.
45. Y. Nam and Y. S. Ju, *J.Adhes.Sci.Technol.*, 2013, **27**, 2163-2176.

Publisher's Note Engineered Science Publisher remains neutral with regard to jurisdictional claims in published maps and institutional affiliations.